Biochemical and Biophysical Research Communications **292,** 702–708 (2002)
doi:10.1006/bbrc.2002.6686, available online at http://www.idealibrary.com on IDEAL®

Prediction of the Tertiary Structure of the β-Secretase Zymogen

Kuo-Chen Chou[1] and W. Jeffrey Howe
Computer-Aided Drug Discovery, Pharmacia & Upjohn, Kalamazoo, Michigan 49007-4940

Received February 28, 2002

β-Secretase, also known as BACE, is a transmembrane aspartyl protease, which generates the N terminus of Alzheimer's disease amyloid β-peptide. The activity of β-secretase is the rate-limiting step of brain plaques production *in vivo,* and hence is a potential target for disease modifying drugs for Alzheimer's disease. To better understand the mechanism of action of β-secretase and help explore novel strategies for drug discovery for Alzheimer's disease, it is important to elucidate the three-dimensional structure of its zymogen. Based on the X-ray structure of the enzyme's protease domain and the X-ray structure of pepsinogen, a model of the three-dimensional structure of the β-secretase zymogen has been constructed. Comparison of the computed structure of pro-BACE with X-ray structures of pepsinogen and progastricsin (two other pro-aspartyl proteases) reveals a significant difference in the relationship of the pro-segment to the catalytic aspartates. In both pepsinogen and progastricsin a lysine side-chain in the pro-segment forms a salt bridge to the two catalytic aspartates, occupying the position normally occupied by a catalytic water. In the pro-BACE model there is no salt bridge, and the corresponding residue—a proline—does not interact at all with the catalytic residues. These findings can be used to elucidate the recent observations that the prodomain of β-secretase does not suppress activity as in a strict zymogen but does appear to facilitate proper folding of an active protease domain. The predicted three-dimensional structure of β-secretase zymogen and the relevant findings might also provide useful insights for rational design of effective drugs against Alzheimer's disease.

Key Words: **human brain memapsin 2; protease domain; pro-peptide; disulfide linkages; aspartyl proteases; salt bridges; catalytic mechanism.**

Alzheimer's disease (AD) is characterized by a neurodegenerative, dementia-inducing disorder that results in a progressive and ultimately fatal loss of mental capacity. The development of AD is accompanied by the gradual spread of sticky plaques and clumps of tangled fibers that disrupt the delicate organization of nerve cells in the brain, undermining the normal communication among brain cells. As brain cells lose ability to communicate with one another, they atrophy—causing memory and reasoning to fade. It is estimated that about 20 million people worldwide (more than 4 million in the United States alone) are suffering from this disease. As the population grows and people live longer, those numbers will increase more than threefold by the year 2050, according to some estimates. Studies in molecular pathology have indicated that the accumulation of the amyloid-β peptide (Aβ), varying in length, but primarily of 40 or 42 amino acids, leads to Aβ fibril deposition or β-sheet (oligomer) amyloid deposition (see, e.g., Ref. 1) in the cerebral cortex of AD patients. Accordingly, the presence of Aβ neuritic plaques is deemed a hallmark of AD and has been suggested to be the cause of all known cases of AD. The formation of Aβ requires two proteolytic cleavages of the membrane-anchored β-amyloid precursor protein (APP). In the nonamyloidogenic pathway APP is cleaved by α-secretase at the sites within the Aβ sequence (2) so as to break it down and prevent the formation of intact Aβ (Fig. 1a); the soluble derivatives thus released are called α-APPs (3). In the amyloidogenic pathway, Aβ is generated from APP by two proteases, the β- and γ-secretases, through the following "aberrant" cellular metabolism of APP: (i) β-secretase cleaves APP at the N-terminus of Aβ peptide (4), generating an APP fragment starting with the first residue of Aβ (Fig. 1b) that is also called β-APP (3) in which Aβ remains intact; (ii) γ-secretase, likely mediated by presenilin 1, cleaves the C terminus of Aβ (3), leading to the complete release of Aβ (Fig. 1c). Therefore, the formation of Aβ, the hallmark of AD, is closely associated with the activities of β-secretase, γ-secretase and/or presenilin. All three enzymes have become po-

Abbreviations used: 3-D, three-dimensional; AD, Alzheimer's disease; APP, amyloid precursor protein; BACE, β-site APP-cleaving enzyme; Aβ, amyloid β-peptide.

[1] To whom correspondence and reprint requests should be addressed. Fax: (616) 372-8766. E-mail: kuo-chen.chou@am.pnu.com.

0006-291X/02 $35.00

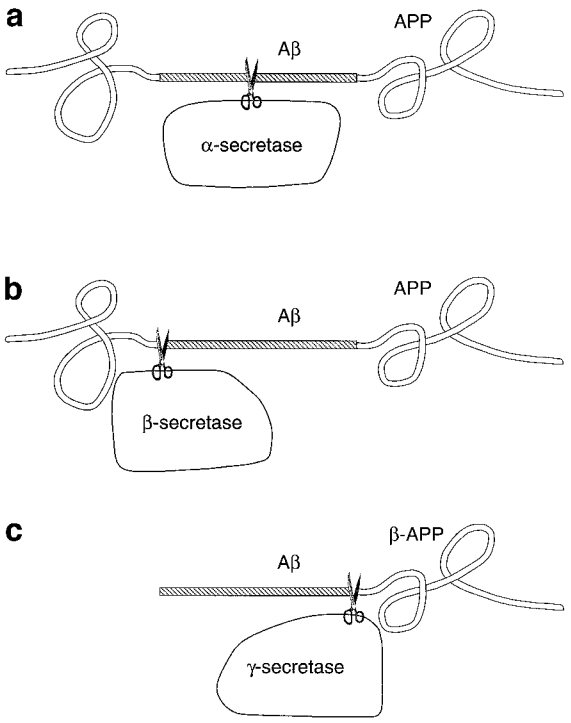

FIG. 1. Schematic drawing to show the normal and abnormal cleavages of APP, where Aβ is shaded to distinguish it from the other part of APP. In the normal case, APP is cleaved by (a) α-secretase at the sites within the Aβ sequence so as to preclude the formation of Aβ. In the abnormal case, APP is cleaved by (b) β-secretase at the N-terminus of Aβ peptide, followed by (c) γ-secretase, likely mediated by presenilin 1, at the C-terminus of Aβ, leading to the complete release of Aβ.

tential targets for inhibitor drugs against AD. The present study is focused on β-secretase. This is because: (i) effective β-secretase cleavage of APP is a prerequisite for formation and secretion of Aβ, and (ii) a 1.9 Å resolution X-ray crystal structure of β-secretase has recently become available (5). Since the formation of Aβ depends on the activity of β-secretase, it is vitally important to reveal the mechanism of the enzyme's activation process. To realize this, it is instructive to develop a 3-D (dimensional) model of the β-secretase zymogen. The present study was initiated in an attempt to find the 3-D structure of β-secretase with its pro-peptide, and to analyze its effect on the function of the enzyme.

MATERIALS AND METHODS

The sequence of the β-secretase zymogen was taken from Vassar *et al.* (6). The sequence alignment for the β-secretase zymogen (abbreviated as pbsz), β-secretase (1fkn), progastricsin (1htr), and pepsinogen (3psg) was performed using the PILEUP program in the GCG package (7). Pepsinogen and progastricsin are pro-enzymes in the family of aspartyl proteases that includes β-secretase. The aligned result is given in Fig. 2, where the pro-peptides are colored blue and the active site residues are red. For the case of pbsz, the signal peptide includes residues 1–21 (not shown), the pro-peptide includes residues 22–45 (8), and the main-chain includes residues 46–446 (with the active site aspartates at 93 and 289). The transmembrane and intracellular domains that follow residue 446 are outside the scope of the current study.

Using the alignment shown in Fig. 2, the 3-D model of the β-secretase zymogen (pbsz) was constructed from (i) the X-ray coordinates of the protease domain of β-secretase (1fkn.pdb) recently determined by Hong *et al.* (5), and (ii) the X-ray coordinates of pepsinogen (3psg.pdb) determined by Hartsuck *et al.* (9). The pro-segment of the pepsinogen structure provided the basis for a homology model of the β-secretase pro-segment, which was grafted onto the β-secretase protease domain, using the procedure described below.

Since the pro-peptide segment and the protease domain of the model were derived from two different templates, an operation for a smooth connection at a proper site (10) for the two structures was needed. This was performed as follows. The template structure 3psg.pdb was superimposed onto the template structure 1fkn.pdb, using the commercial software package, MOE (Chemical Computing Ltd.). During the superimposition process the entire structure of 3psg underwent a translational and rotational motion (11), and hence the coordinates of 3psg changed, although the coordinates of 1fkn remained unchanged. It was observed from the superimposed pair that, starting from Gly-74 and proceeding in the C-terminal direction (the residue number is counted based on the sequence of pbsz as shown in Fig. 2), the backbone chain of 1fkn followed almost the same trajectory as that of the backbone chain of 3psg, for most of the N-terminal lobe of the bilobal structures. Moving in the N-terminal direction from Gly-74 of β-secretase, however, the structures diverged markedly. Accordingly, residues 74 of the β-secretase structure became the joining point for grafting on the pro-segment of pepsinogen (in the form of the actual β-secretase pro-segment sequence). A smooth connection between residues 16–72 of 3psg and residues 74–446 of 1fkn (Fig. 2) was realized without causing any structural conflicts. The structure thus obtained was then used as a combined template to develop the final 3-D model of the β-secretase zymogen (pbsz) by the segment matching modeling method (12).

The segment matching approach (in the MOE software) employs a database of known protein structures to build an unknown target structure based on an amino acid sequence alignment. In this case the target structure was the β-secretase zymogen, i.e., the pro-segment plus the protease domain of β-secretase. The target structure was first broken into a set of short segments. The database was then searched for matching segments on the basis of amino acid sequence similarity and compatibility with the target structure. The process was repeated 10 times and an average model was generated, followed by energy minimization of the entire pro-enzyme to create the final model. The structure thus obtained uniquely defined the atomic coordinates of not only residues 22–45, the pro-segment of pbsz, but also the segment of residues 46–55 in the main chain that was missing in the crystal structure of 1fkn.pdb (5). Furthermore, although the majority of the protease domain (residues 75–446) of pbsz was almost identical to the corresponding sequence in 1fkn, a small transition-linking part of the protease domain (residues 56–74) was affected owing to the existence of the pro-segment. This procedure was originally shown to be highly accurate for eight test proteins ranging in size from 46 to 323 residues, where the all-atom root-mean-square deviation (RMSD) of the modeled structures was between 0.93 and 1.73 Å (12). This method was previously used to model the structure of the protease domain of caspase-8, at a time before the X-ray coordinates were released for caspase-3 (13). In that particular study, the atomic coordinates of the catalytic domain of caspase-3 were predicted based on the X-ray structure of caspase-1, and then the caspase-3 structure thus obtained served as a template to model the protease domain of caspase-8. After the X-ray coordinates of caspase-3 protease domain were finally released and the X-ray structure of the caspase-8 protease domain was determined (14), it turned out that the RMSD for all the backbone atoms of the

FIG. 2. Sequence alignment of β-secretase zymogen (pbsz), β-secretase (1fkn), progastricsin (1htr) and pepsinogen (3psg), where the X-ray structures for 1fkn, 1htr, and 3psg are known, and the structure for pbsz is to be predicted. The pro-peptides are colored blue. The yellow line indicates the residue pair involved in forming disulfide bond as observed in 1fkn. The codes in red bold type represent the conserved residues at the active site for the aspartyl protease family. Their sequence locations are residues 93–95 and residues 289–291 for pbsz, residues 91–93 and residues 274–276 for 3psg, and residues 91–93 and residues 276–278 for 1htr. See text for further explanation. The signal peptide segments (residues 1–21 for pbsz, residues 1–16 for 1htr, and residues 1–15 for 3psg) were not included for the alignment operation because they will be cleaved off by signal peptidase during the secretory process (see, e.g., (24)).

caspase-3 protease domain between the X-ray and predicted structures was 2.7 Å, while the corresponding RMSD was 3.1 Å for caspase-8, and only 1.2 Å for its core structure. This indicates that the computed structures of caspase-3 and -8 were quite close to the corresponding X-ray structures. Later on, this method was successively applied to model the CARDs (caspase recruitment domains) of

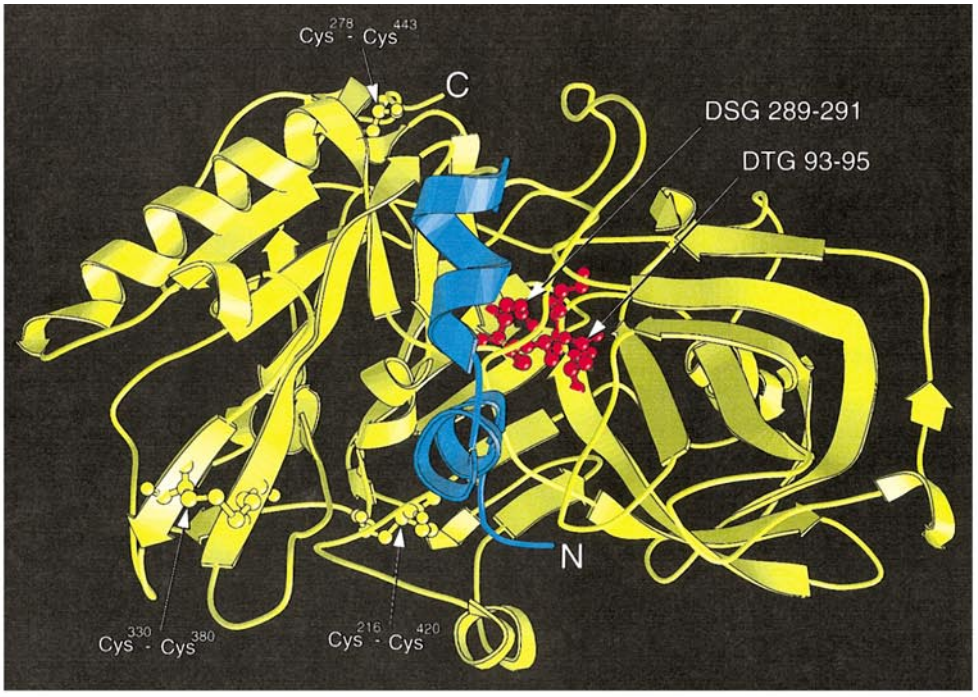
Cys278 - Cys443
C
DSG 289-291
DTG 93-95
N
Cys330 - Cys380
Cys216 - Cys420

3

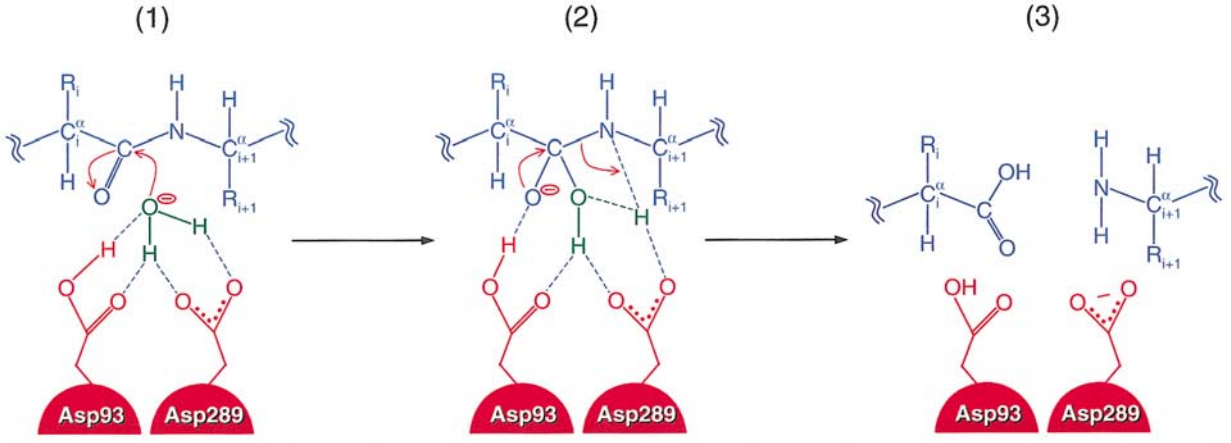
(1)
(2)
(3)
Asp93
Asp289
Asp93
Asp289
Asp93
Asp289

4

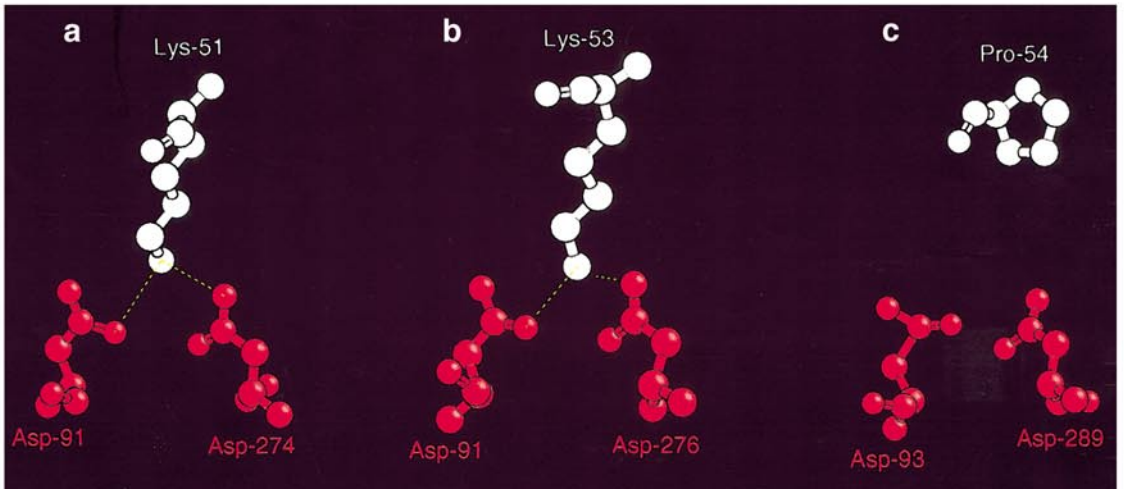
a
Lys-51
Asp-91
Asp-274
b
Lys-53
Asp-91
Asp-276
c
Pro-54
Asp-93
Asp-289

5

Apaf-1, Ced-4 and Ced-3, based on the NMR structure of the RAIDD CARD (15), and to model the Cdk5-P35 complex (16) as well as the protease domain of caspase-9 (17).

RESULTS AND DISCUSSION

The predicted 3-D structure thus obtained for the β-secretase zymogen is illustrated in Fig. 3. The pro-peptide segment (residues 25–45) is colored blue, the main chain colored yellow, and the active site residues (DTG 93–95, DSG 289–291) are colored red. The resulted 3-D model provides us with a detailed look at the structural relationship between the active site of the enzyme and its pro-peptide segment.

1. Overall structure. Since the origins of the protease domain of the model came from crystallographic coordinates, it was expected that the final energy minimized model of that domain would retain most, if not all, of the experimental attributes, and that was the case. In particular, the model retained the three pairs of disulfide bonds, i.e., Cys^{216}–Cys^{420}, Cys^{278}–Cys^{443}, and Cys^{330}–Cys^{380}. This implies that the existence of the pro-peptide segment would not destroy the disulfide bonds but rather likely facilitate a proper folding for forming the three pairs disulfide bonds as observed in an active protease domain (18). Proceeding in the N-terminal direction from the pro-segment attachment point, the backbone traces a path from one end of the active site cleft, toward the center, then covers over the "flap" of the active site as described in (5). It then continues toward the far end of the active site, makes a turn, and returns via two helices to near its origination point. Its overall structure is somewhat similar to the pepsinogen pro-segment from which it was derived, but with a key difference described below. An overlay of the β-secretase crystal structure with the pro-enzyme model shows some differences in side chain positioning induced by the presence of the pro-segment, and very minor differences in distal positioning, likely due to the energy minimization.

2. The effect of the pro-peptide to the activity of β-secretase. Generally speaking, an enzyme will be inactivated by the existence of its pro-peptide. However, unlike the case of most other zymogens, the existence of the pro-peptide does not seem to have a significant impact on the activity of β-secretase. This can be elucidated as follows. Inactivation of an enzyme by its pro-peptide is generally thought to be due to physical blockage of the catalytic site, preventing access to substrate. In the case of aspartyl proteases, a pro-segment could also disrupt the catalytically-required water molecule between the two aspartates.

A comparison of the 3-D structures of pepsinogen, pro-gastricsin, and the β-secretase pro-enzyme model indicates that the pro-segments of all three cover up the catalytic site, and therefore should block access to substrate. The dynamics of protein motion, however, could allow periodic unfolding of the pro-segments exposing the catalytic clefts to enable substrate processing. Yet only for the β-secretase pro-enzyme is substrate processing known to occur, so there is something unique about the positioning of its pro-segment.

As mentioned above, the substrate amide bond hydrolysis by aspartyl proteases requires the participation of a water molecule (19), as illustrated in Fig. 4. The catalytic reaction involves (i) the β-carboxyl groups of the two Asp residues (i.e., Asp-93 and Asp-289 for the case of β-secretase) at the active site being brought in to close proximity to activate a water molecule by forming hydrogen bonds with it; (ii) the nucleophilic attack of the activated water molecule on the carbonyl carbon atom of the scissile peptide bond to form the tetrahedral intermediate; (iii) the decomposition of the tetrahedral intermediate to yield the product of cleaved peptides and active enzyme. Accordingly, before a peptide bond is cleaved by an aspartyl protease, the two Asp residues at the active site must first activate a water molecule by forming four hydrogen bonds with it.

However, for the case of pepsinogen (3psg), the two active site Asp residues, i.e., Asp-91 and Asp-274 (Fig. 2), have already bonded to Lys-51 of the pro-peptide by two salt bridges: one is between $O^{\delta 1}$ of Asp-91 and N^{ζ} of Lys-51, and the other between $O^{\delta 2}$ of Asp-274 and N^{ζ} of Lys-51 (Fig. 5a), as clearly shown in the X-ray struc-

FIG. 3. The computed structure of β-secretase zymogen based on the sequence alignment of Fig. 2. The pro-peptide segment is colored light blue, the protease domain is colored yellow, and the active site (DTG 93–95, DSG 289–291) is colored red. The residues involved in forming three disulfide bonds are shown with the ball-and stick drawing.

FIG. 4. The catalytic mechanism of β-secretase. In abridged form, the reaction involves (1) the β-carboxyl groups of the two active site Asp residues, Asp-93 and Asp-289, being brought in to close proximity to activate a water molecule by forming four hydrogen bonds with it; (2) the nucleophilic attack of the activated water molecule on the carbonyl carbon atom of the scissile peptide bond to form the tetrahedral intermediate; (3) the decomposition of the tetrahedral intermediate to yield the cleaved peptide product and active enzyme. The red arrows between atoms approximate the bond-forming and -breaking process. By modifying the sequence number of the two active site Asp residues, the schematic drawing can be used to illustrate the catalytic mechanism of all the other aspartyl proteases as well.

FIG. 5. A ball-and-stick drawing to highlight the interaction of the two active site Asp residues with the closest residue from the pro-peptide. Only heavy atoms are shown. (a) For the case of pepsinogen (3psg), Asp-91 and Asp-274 are bonded to Lys-51 of the pro-peptide by two salt bridges (dash line): one is between $O^{\delta 1}$ of Asp-91 and N^{ζ} of Lys-51, and the other between $O^{\delta 2}$ of Asp-274 and N^{ζ} of Lys-51. (b) For the case of progastricsin (1htr), Asp-91 and Asp-276 are bonded to Lys-53 by two salt bridges: one is between $O^{\delta 1}$ of Asp-91 and N^{ζ} of Lys-53, and the other between $O^{\delta 2}$ of Asp-276 and N^{ζ} of Lys-53. (c) For the case of the β-secretase zymogen model, no salt-bridge can be formed between the active site Asp residues and Pro-54, the residue corresponding to the Lys locations in the other two pro-enzyme structures (Fig. 2).

ture determined by Hartsuck *et al.* (9). As is well known, salt-bridges are stronger than hydrogen bonds (see, e.g., (20)). This will certainly disrupt the two active site Asp residues in activating a water molecule, and hence the activity of the pepsinogen in cleaving a peptide bond is impeded by the existence of the pro-peptide segment. A similar situation also occurs in the case of progastricsin (1htr), where the two active site Asp residues, i.e., Asp-91 and Asp-276, have also formed two salt bridges with Lys-53 of the pro-peptide: one is between $O^{\delta 1}$ of Asp-91 and N^{ζ} of Lys-53, and the other between $O^{\delta 2}$ of Asp-276 and N^{ζ} of Lys-53 (Fig. 5b), as shown by the X-ray structure determined by Ivanov *et al.* (21). Accordingly, one could view the salt bridges to the aspartates as a "locking" mechanism that holds the pro-segment in place and prevents the proper positioning of a catalytic water molecule.

The microenvironment is much different in the β-secretase zymogen model, where no salt bridges whatsoever are observed between the pro-peptide segment and the two active site Asp residues, i.e., Asp-93 and Asp-289 (Fig. 2). According to the model, it is Pro-54 that corresponds to the Lys locations in the other two pro-enzyme structures from both sequence alignment (Fig. 2) and 3-D structure (Fig. 5c). However, a proline side-chain cannot form a salt-bridge. Thus, for the case of the β-secretase zymogen, the "locking" mechanism is absent and there is no pro-segment side-chain in the location of the catalytic water position.

According to this model, therefore, the existence of the pro-peptide segment should not completely reduce the activity of β-secretase. This structural observation is supported by the recent experimental observations from the following two independent groups. Shi *et al.* (22) observed that, when assayed with a polypeptide substrate, the k(cat)/K(m) of β-secretase with the pro-segment intact is only 2.3-fold less than β-secretase. They concluded that the pro-domain of β-secretase "does not suppress activity as in a strict zymogen but does appear to facilitate proper folding of an active protease domain." Benjannet *et al.* (23) observed that "pro-BACE can produce significant quantities of Swedish mutant βAPP_{sw} β-secretase product C99," and hence the pro-domain has little effect on the BACE active site.

While the absence of the "locking mechanism" in the pro-BACE model provides a possible explanation for the unusual retained activity of the pro-enzyme, the design of experiments to test the hypothesis is complicated by the fact that Pro-54 in the pro-BACE model imparts a substantially different backbone trajectory in the region of that residue, compared to what is observed in the two comparator crystal structures (3psg and 1htr). This observation would be expected, due to the cyclic conformational constraints of a proline. Mutation of the proline to a lysine in pro-BACE would, correspondingly, also be expected to change the backbone characteristics in that region. In fact, we have found that such a single mutation is insufficient to reduce or eliminate activity of the pro-enzyme (Mildner, A. M., Tomasselli, A. G., and Heinrickson, R. L., unpublished results). This suggests that confirmation of the hypothesis by experimental modification of the BACE pro-segment would need to involve more than just the Pro54Lys mutation, to include one or more additional residues that would enable the nearby pro-segment backbone to more closely mimic those of the comparator pro-enzymes.

Although computer-predicted protein structures are still not as accurate as X-ray structures, modeled structures such as the one presented here can be used to understand and test hypotheses about biological function. Particularly, the present model provides novel insights into molecular mechanisms that can be used to address why the pro-domain of β-secretase does not confer strict zymogen-like properties. Since β-secretase purportedly plays a pivotal role in the etiology of Alzheimer's disease and has become an important target for inhibitor drugs against Alzheimer's disease, the 3-D structure of the β-secretase zymogen and the relevant findings as revealed here should provide useful insights in modulating the activity of the enzyme and encourage the development of novel strategies to prevent the production of Aβ.

ACKNOWLEDGMENTS

The authors thank Raymond B. Moeller, Cynthia A. Ludlow, Wendy Vanderheide, and Katie Crawford of Pharmacia's Graphic Service Group for their help of drawing the figures in this paper. Valuable discussions with Alfredo G. Tomasselli, Robert L. Heinrikson, and Timothy E. Benson are also gratefully acknowledged. We especially thank Dr. Heinrikson and colleagues for carrying out a mutational experiment suggested by this work.

REFERENCES

1. Carter, D. B., and Chou, K. C. (1998) *Neurobiol. Aging* **19,** 37–40.
2. Haass, C., and Selkoe, D. J. (1993) *Cell* **75,** 1039–1042.
3. Wolfe, M. S., Xia, W., Ostaszewski, B. L., Diehl, T. S., Kimberly, W. T., and Selkoe, D. J. (1999) *Nature* **398,** 513–517.
4. Sinha, S., and Lieberburg, I. (1999) *Proc. Natl. Acad. Sci. USA* **96,** 11049–11503.
5. Hong, L., Koelsch, G., Lin, X., Wu, S., Terzyan, S., Ghosh, A. K., Zhang, X. C., and Tang, J. (2000) *Science* **290,** 150–153.
6. Vassar, R., Bennett, B. D., Babu-Khan, S., Kahn, S., Mendiaz, E. A., Denis, P., Teplow, D. B., Ross, S., Amarante, P., Loeloff, R., Luo, Y., Fisher, S., Fuller, J., Edenson, S., Lile, J., Jarosinski, M. A., Biere, A. L., Curran, E., Burgess, T., Louis, J.-C., Collins, F., Treanor, J., Rogers, G., and Citron, M. (1999) *Science* **286,** 735–741.
7. Devereux, J. (1994) *in* Genetic Computer Group, Madison, Wisconsin.
8. Bennett, B. D., Denis, P., Haniu, M., Teplow, D. B., Kahn, S., Louis, J.-C., Citron, M., and Vassar, R. (2000) *J. Biol. Chem.* **275,** 37712–37717.

9. Hartsuck, J. A., Koelsch, G., and Remington, S. J. (1992) *Proteins Struct. Funct. Genet.* **13,** 1–25.
10. Chou, K. C., Nemethy, G., Pottle, M., and Scheraga, H. A. (1989) *J. Mol. Biol.* **205,** 241–249.
11. Chou, K. C., Pottle, M., Nemethy, G., Ueda, Y., and Scheraga, H. A. (1982) *J. Mol. Biol.* **162,** 89–112.
12. Levitt, M. (1992) *J. Mol. Biol.* **226,** 507–533.
13. Chou, K. C., Jones, D., and Heinrikson, R. L. (1997) *FEBS Lett.* **419,** 49–54.
14. Watt, W., Koeplinger, K. A., Mildner, A. M., Heinrikson, R. L., Tomasselli, A. G., and Watenpaugh, K. D. (1999) *Structure* **7,** 1135–1143.
15. Chou, J. J., Matsuo, H., Duan, H., and Wagner, G. (1998) *Cell* **94,** 171–180.
16. Chou, K. C., Watenpaugh, K. D., and Heinrikson, R. L. (1999) *Biochem. Biophys. Res. Commun.* **259,** 420–428.
17. Chou, K. C., Tomasselli, A. G., and Heinrikson, R. L. (2000) *FEBS Lett.* **470,** 249–256.
18. Haniu, M., Denis, P., Young, Y., Mendiaz, E. A., Fuller, J., Hui, J. O., Bennett, B. D., Kahn, S., Ross, S., Burgess, T., Katta, V., Rogers, G., Vassar, R., and Citron, M. (2000) *J. Biol. Chem.* **275,** 21099–21106.
19. Silverman, R. B. (2000) The Organic Chemistry of Enzyme-Catalyzed Reactions, Chap. 2, Academic Press, San Diego.
20. Schulz, G. E., and Schirmer, R. H. (1979) Principles of Protein Structure, Chap. 3, Springer-Verlag, New York.
21. Ivanov, P. K., Chernaia, M., Gustchina, A. E., I. V., P., Nikonov, S. V., and Tarasova, H. I. (1990) *Biochim. Biophys. Acta* **1040,** 308–310.
22. Shi, X. P., Chen, E., Yin, K. C., Na, S., Garsky, V. M., Lai, M. T., Li, Y. M., Platchek, M., Register, R. B., Sardana, M. K., Tam, M. J., Thiebeau, J., Wood, T., Shafer, J. A., and Gardell, S. J. (2001) *J. Biol. Chem.* **276,** 10366–10373.
23. Benjannet, S., Elagoz, A., Wickham, L., Mamarbachi, M., Munzer, J. S., Basak, A., Lazure, C., Cromlish, J. A., Sisodia, S., Checler, F., Chrétien, M., and Seidah, N. G. (2001) *J. Biol. Chem.* **276,** 10879–10887.
24. Chou, K. C. (2001) *Protein Eng.* **14,** 75–79.